Widespread Translational Inhibition by Plant miRNAs and siRNAs

Peter Brodersen, *et al.*

Science **320**, 1185 (2008);
DOI: 10.1126/science.1159151

Science (print ISSN 0036-8075; online ISSN 1095-9203) is published weekly, except the last week in December, by the American Association for the Advancement of Science, 1200 New York Avenue NW, Washington, DC 20005.

found that they generated too much deflection (see SOM text and fig. S5). This is an alternative way of arriving at the conclusion that Mars probably has subchondritic heat sources.

References and Notes

1. K. R. Blasius, J. A. Cutts, A. D. Howard, *Icarus* **50**, 140 (1982).
2. J. A. Cutts, B. H. Lewis, *Icarus* **50**, 216 (1982).
3. P. C. Thomas, S. W. Squyres, K. E. Herkenhoff, A. D. Howard, B. C. Murray, in *Mars*, H. H. Kieffer, B. M. Jakosky, C. W. Snyder, M. S. Matthews, Eds. (Univ. of Arizona Press, Tucson, AZ, 1992), pp. 767–795.
4. M. C. Malin, K. S. Edgett, *J. Geophys. Res.* **106**, 23429 (2001).
5. K. E. Fishbaugh, J. W. Head, *Icarus* **174**, 444 (2005).
6. S. Byrne, B. C. Murray, *J. Geophys. Res.* **107**, 5044 (2002).
7. K. S. Edgett, R. M. E. Williams, M. C. Malin, B. A. Cantor, P. C. Thomas, *Geomorphology* **52**, 289 (2003).
8. K. L. Tanaka *et al.*, *Icarus*, published online 29 February 2008; 10.1016/j.icarus.2008.01.021.
9. K. E. Herkenhoff, S. Byrne, P. S. Russell, K. E. Fishbaugh, A. S. McEwen, *Science* **317**, 1711 (2007).
10. Features in the radargram beneath the troughs may or may not be real structures. The discontinuities in reflections might arise, for example, from poor radar-signal penetration because of surface scattering from the trough floors.
11. G. Picardi *et al.*, *Science* **310**, 1925 (2005), published online 29 November 2005; 10.1126/science.1122165.
12. W. M. Calvin *et al.*, *Lunar Planet. Sci.* **XXXIX**, 1939 (abstr.) (2008).
13. Y. Langevin *et al.*, *Science* **307**, 1581 (2005), published online 17 February 2005; 10.1126/science.1109438.
14. M. T. Zuber *et al.*, *Science* **317**, 1718 (2007).
15. D. C. Nunes, R. J. Phillips, *J. Geophys. Res.* **111**, E06S21 (2006).
16. J. Laskar, B. Levrard, J. F. Mustard, *Nature* **419**, 375 (2002).
17. The climate precession is the insolation effect of the precession of the spin axis modulated by the orbital eccentricity. The result is that the calendar date of perihelion precesses.
18. M. T. Mellon, B. M. Jakosky, *J. Geophys. Res.* **100**, 11781 (1995).
19. B. Levrard, F. Forget, F. Montmessin, J. Laskar, *J. Geophys. Res.* **112**, E06012 (2007).
20. S. M. Milkovich, J. W. Head III, *J. Geophys. Res.* **110**, E01005 (2005).
21. R. M. Haberle, J. R. Murphy, J. Schaeffer, *Icarus* **161**, 66 (2003).
22. O. B. Toon, J. B. Pollack, W. Ward, J. A. Burns, K. Bilski, *Icarus* **44**, 552 (1980).
23. J. Laskar *et al.*, *Icarus* **170**, 343 (2004).
24. W. B. Banerdt, *J. Geophys. Res.* **91**, 403 (1986).
25. C. L. Johnson *et al.*, *Icarus* **144**, 313 (2000).
26. J. J. Plaut *et al.*, *Science* **316**, 92 (2007), published online 14 March 2007; 10.1126/science.1139672.
27. M. A. Wieczorek, *Icarus*, published online 10 January 2008; 10.1016/j.icarus.2007.10.026.
28. M. Grott, D. Breuer, *Icarus* **193**, 503 (2008).
29. M. K. McNutt, *J. Geophys. Res.* **89**, 11180 (1984).
30. S.-i. Karato, P. Wu, *Science* **260**, 771 (1993).
31. S. A. Hauck II, R. J. Phillips, *J. Geophys. Res.* **107**, 5052 (2002).
32. Y. Caristan, *J. Geophys. Res.* **87**, 6781 (1982).
33. V. Belleguic, P. Lognonné, M. Wieczorek, *J. Geophys. Res.* **110**, E11005 (2005).
34. C. L. Johnson, R. J. Phillips, *Earth Planet. Sci. Lett.* **230**, 241 (2005).
35. D. Breuer, T. Spohn, *J. Geophys. Res.* **108**, 5072 (2003).
36. P. S. Mohit, R. J. Phillips, *J. Geophys. Res.* **111**, E12001 (2006).

37. SHARAD was provided by the Italian Space Agency, and its operations are led by Dipartimento InfoCom, Università di Roma "La Sapienza." Thales Alenia Space Italia is the prime contractor for SHARAD. The Mars Reconnaissance Orbiter mission is managed by the Jet Propulsion Laboratory, California Institute of Technology, for the NASA Science Mission Directorate, Washington, DC. Lockheed Martin Space Systems, Denver, CO, is the prime contractor for the orbiter. We thank three anonymous reviewers for very constructive comments. S. Hauck provided very useful advice.

Supporting Online Material

www.sciencemag.org/cgi/content/full/1157546/DC1
Materials and Methods
Figs. S1 to S5
References

10 March 2008; accepted 7 May 2008
Published online 15 May 2008;
10.1126/science.1157546
Include this information when citing this paper.

Widespread Translational Inhibition by Plant miRNAs and siRNAs

Peter Brodersen,[1] Lali Sakvarelidze-Achard,[1] Marianne Bruun-Rasmussen,[1] Patrice Dunoyer,[1] Yoshiharu Y. Yamamoto,[2] Leslie Sieburth,[3] Olivier Voinnet[1]*

High complementarity between plant microRNAs (miRNAs) and their messenger RNA targets is thought to cause silencing, prevalently by endonucleolytic cleavage. We have isolated *Arabidopsis* mutants defective in miRNA action. Their analysis provides evidence that plant miRNA–guided silencing has a widespread translational inhibitory component that is genetically separable from endonucleolytic cleavage. We further show that the same is true of silencing mediated by small interfering RNA (siRNA) populations. Translational repression is effected in part by the ARGONAUTE proteins AGO1 and AGO10. It also requires the activity of the microtubule-severing enzyme katanin, implicating cytoskeleton dynamics in miRNA action, as recently suggested from animal studies. Also as in animals, the decapping component VARICOSE (VCS)/Ge-1 is required for translational repression by miRNAs, which suggests that the underlying mechanisms in the two kingdoms are related.

MicroRNAs are 20- to 24-nucleotide (nt) RNAs that regulate eukaryotic gene expression posttranscriptionally. Bound to ARGONAUTE (AGO) proteins, miRNAs guide RNA-induced silencing complexes (RISCs) to partly or fully complementary mRNAs (*1*). Two modes of negative regulation by RISC exist: (i) translational repression, sometimes coupled to accelerated mRNA decay, and (ii) RISC-catalyzed endonucleolytic mRNA cleavage ("slicing"). The degree of miRNA-mRNA complementarity is a key determinant of the mechanism used, such that perfect complementarity enables cleavage, whereas central mismatches exclude slicing to promote translational repression (*2*, *3*). Unlike most animal miRNAs, most plant miRNAs show near-perfect or perfect complementarity to their targets, and slicing is believed to be their predominant, or exclusive, mode of action (*4*). Accordingly, *Arabidopsis* AGO1 binds miRNAs and displays slicer activity toward miRNA targets, and strong *ago1* loss-of-function mutants overaccumulate miRNA target transcripts (*5*–*7*). Nonetheless, many questions regarding miRNA-RISC composition, loading, and target identification persist, mostly because AGO1 remains the only factor known to be implicated in plant miRNA action. It is also unclear whether near-perfect complementarity within plant miRNA–target pairs actually excludes translational inhibition, as is commonly inferred, or whether it allows slicing to occur in addition to translational inhibition.

To address these issues, we carried out a forward genetic screen for *Arabidopsis* mutants defective in silencing of a constitutively expressed green fluorescent protein (GFP) mRNA containing a miR171 target site immediately downstream of the stop codon (Fig. 1A) (*8*). In seedlings, GFP is silenced by endogenous miR171, except in the vasculature and in the roots where miR171 expression is low (*8*). Twenty-one recessive mutants defective in miR171-guided silencing were identified by gain of GFP expression in leaves (Fig. 1B); none had mutations in the miR171 target site. Eight nonallelic mutants showing consistently higher GFP expression than the parental line GFP171.1 [wild type (WT)] after two backcrosses (fig. S1) were studied in further detail.

***mbd* and *mad* mutants.** Two mutants (class I) had strongly reduced levels of several miRNAs and were referred to as *microRNA biogenesis deficient* (*mbd1* and *mbd2*) (fig. S1 and Fig. 1C). miRNA biogenesis in *Arabidopsis* involves processing of primary miRNA transcripts by a nuclear-localized complex of DICER-LIKE1 (DCL1), the double-stranded RNA binding protein HYL1, and the zinc finger protein SE. Excised miRNA/miRNA* duplexes are then stabilized through HEN1-catalyzed 2′-O-methylation [reviewed in (*9*)]. A G-to-A transition in *mbd1* (renamed *dcl1-12*) disrupts a splice donor site in the *DCL1* gene, which strongly reduces the accumulation of correctly spliced DCL1 mRNA (fig. S1). *mbd2* (renamed *hen1-7*) has a missense mutation resulting in a Gly-to-Glu change in the HEN1 *S*-adenosyl methionine–binding motif, which is predicted to abolish small RNA methylation (fig. S1). The remaining six mutants exhibited normal miRNA levels and were classified as *microRNA action deficient mad1* to *mad6* (Fig. 1C). *mad1* to *mad6* showed low miR160*

[1]Institut de Biologie Moléculaire des Plantes du CNRS, Unité Propre de Recherche 2357, 12 rue du Général Zimmer, 67084 Strasbourg Cedex, France. [2]Center for Gene Research, Nagoya University, Furo-cho, Chikusa-ku, Nagoya Aichi, 464-8602, Japan. [3]Department of Biology, University of Utah, Salt Lake City, UT 84112, USA.

*To whom correspondence should be addressed. E-mail: olivier.voinnet@ibmp-ulp.u-strasbg.fr

accumulation, indicating intact strand separation and miRNA* degradation (Fig. 1C). All *mad* mutants map to loci not previously implicated in RNA silencing (table S1). Thus, our screen identifies known miRNA biogenesis genes and unknown factors required for miRNA action.

Two classes of *mad* mutants. Because miR171 is perfectly complementary to its target site and guides slicing (*8*, *10*), GFP mRNA levels were expected to be elevated in *mad* mutants as compared with WT plants. Indeed, *dcl1-12*, *hen1-7*, and *mad1* to *mad4* mutants exhibited higher levels of GFP mRNA and protein than WT plants, whereas the mRNA and protein levels of the non-miRNA target Hsc70 were unchanged (Fig. 2, A and B). The elevated GFP mRNA levels resulted from defective slicing, because the ratios of GFP full-length mRNA to GFP 3′-cleavage fragments were higher than in WT plants (fig. S1). By contrast, *mad5* and *mad6* mutants had low GFP mRNA levels similar to those in WT plants, yet had much higher GFP protein levels (Fig. 2, A and B, and fig. S1). The overaccumulation of GFP protein was specifically due to defective miR171-directed repression because an mRNA lacking the miR171 target site ($GFP_{no\ miR}$) produced similar GFP levels in *mad5*, *mad6*, and WT plants (Fig.

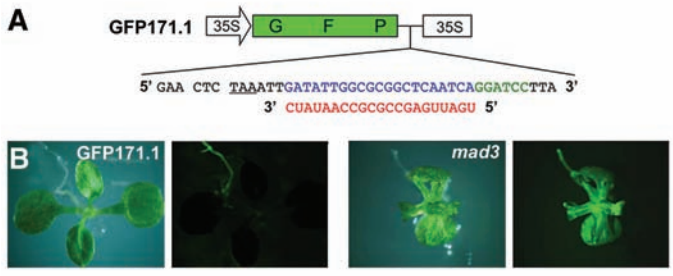

Fig. 1. Isolation of *mbd* and *mad* mutants. (**A**) Schematic representation of the GFP171.1 construct reporting miR171 activity. The miR171 target sequence was inserted downstream of the stop codon (underlined). (**B**) Example of loss of GFP silencing in a *mad* mutant (*mad3*, 15 days of growth). From left to right, the first and third images are in transmitted light, whereas the second and fourth images show GFP fluorescence upon blue light excitation. (**C**) Northern analysis of distinct miRNAs (top panels) and comparison of miR160 and miR160* accumulation (bottom panels). RNA from transgenic seedlings expressing the tombusviral P19 protein, which sequesters small RNA duplexes, provides a positive control for miRNA* overaccumulation.

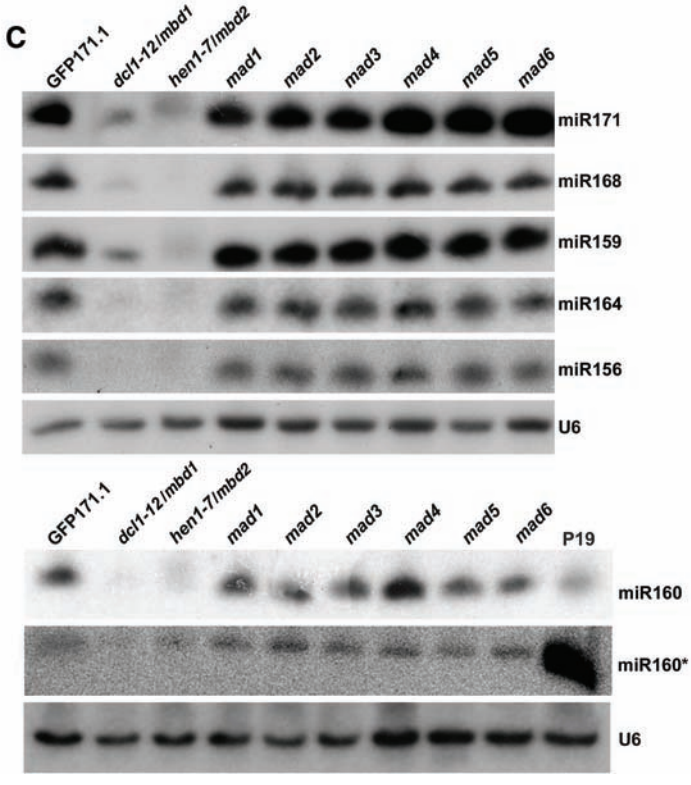

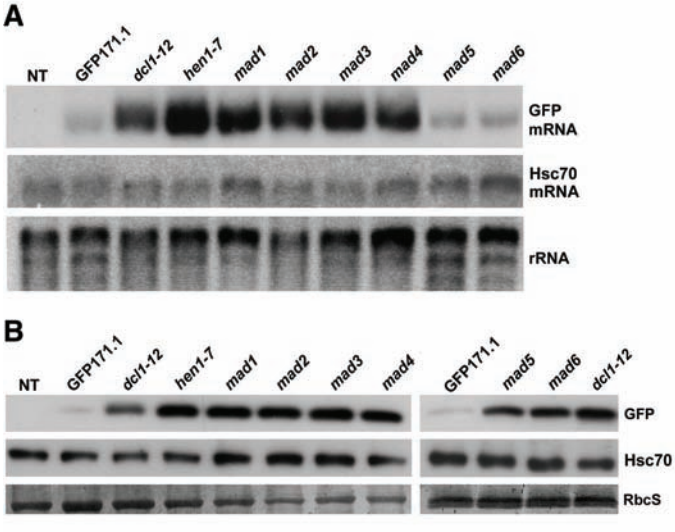

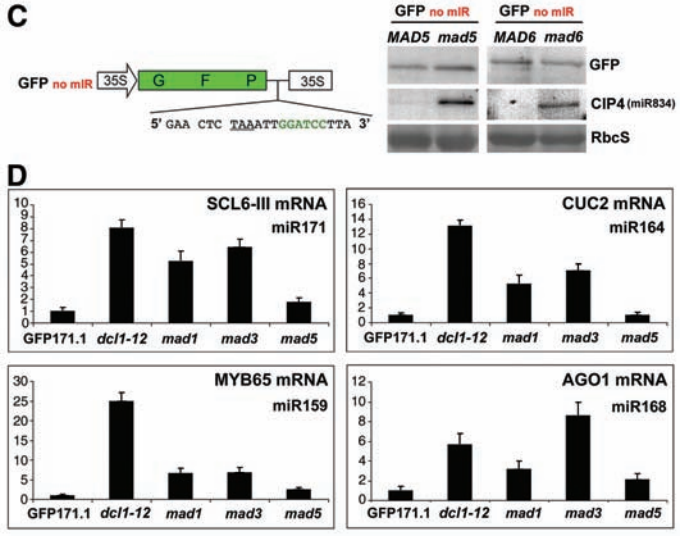

Fig. 2. Molecular analysis of mutants. (**A**) RNA blot analysis with GFP- and Hsc70-specific probes. Ribosomal RNA (rRNA) was stained with ethidium bromide. NT, nontransgenic WT plant. (**B**) Western analysis of GFP and Hsc70. Coomassie-stained RbcS provides a loading control. (**C**) Representation of the $GFP_{no\ miR}$ transgene devoid of a miR171 target site and GFP protein accumulation from $GFP_{no\ miR}$ introduced into *mad5* and *mad6* by crossing (see the SOM materials and methods). Differential accumulation of CIP4 (miR834 target) confirms the presence of the mutations (Fig. 3E). (**D**) Quantitative RT-PCR analysis of mRNA accumulation of four endogenous miRNA targets. cDNA inputs were normalized to 18S rRNA, and expression ratios for each mRNA are given relative to the level in the GFP171.1 parental line. Data are displayed as averages ± SD (n = 3 PCR replicates).

2C). Accordingly, accumulation of the non-miRNA targets RbcS, HSC70 (Fig. 2B), and CDC2A (fig. S1) was unchanged in the two mutants as compared with WT plants. Quantitative reverse transcription polymerase chain reaction (RT-PCR) analyses of representative mutants revealed that *mad1* and *mad3* overaccumulate endogenous transcripts known to be targeted by miRNAs other than miR171, whereas little or no difference was observed in *mad5* (Fig. 2D). These data indicate that *mad1*→*mad4* mutants carry lesions in genes required for miRNA-guided transcript degradation (class II mutants). By contrast, miRNA-guided slicing occurs normally in *mad5* and *mad6* (class III mutants), yet both fail to silence the synthetic GFP171.1 target at the protein level. We propose that the low GFP accumulation in the transgenic line GFP171.1 is due to at least two distinct mechanisms mediated by the perfectly complementary miR171: (i) slicing leading to reduced transcript levels and (ii) inhibition of protein production from the remaining unsliced mRNAs. We further propose that class III mutants are specifically defective in the second process.

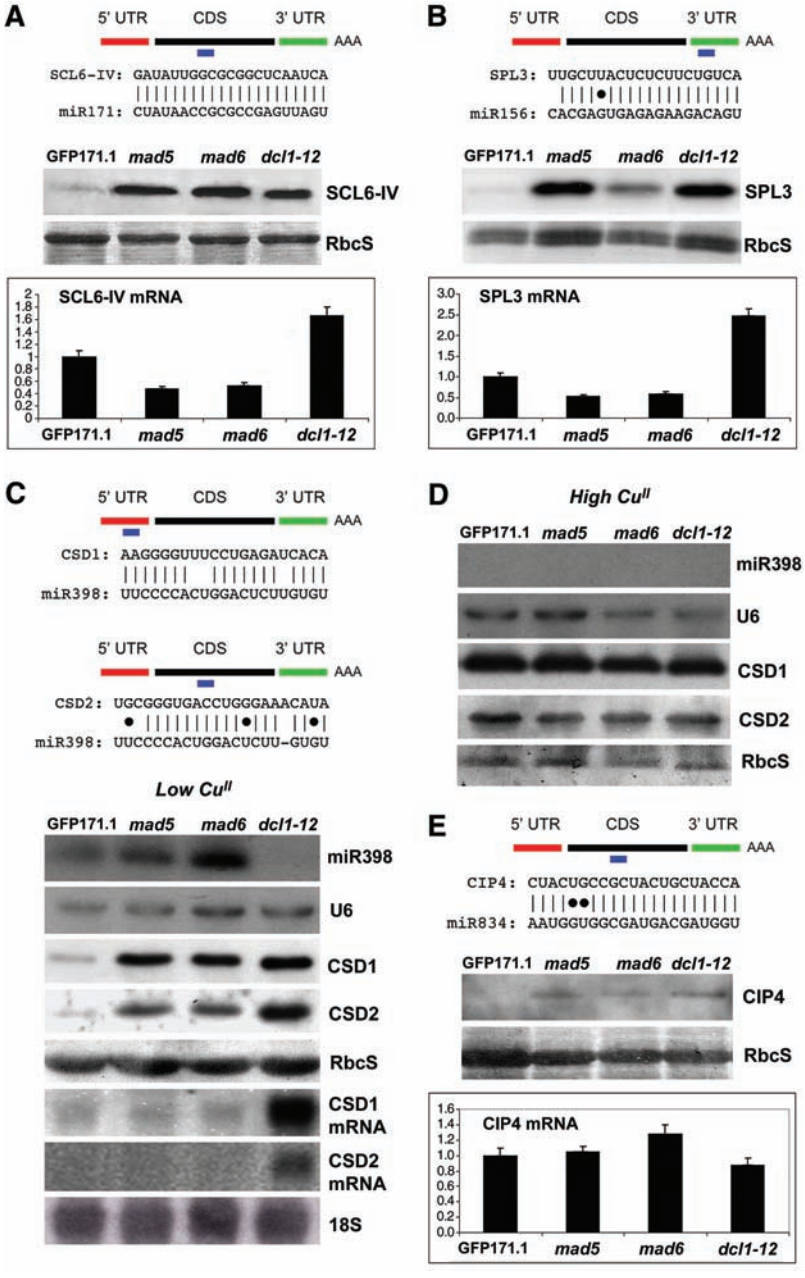

Fig. 3. miRNA target protein and mRNA accumulation in *mad5* and *mad6* mutants. Target site positions and miRNA-mRNA complementarities are shown. (**A**) Western and real-time RT-PCR analyses of SCL6-IV protein and mRNA, as in Fig. 2D. (**B**) SPL3 protein and mRNA analyzed as in (A). (**C**) mRNA and protein accumulation of the miR398 targets CSD1 and CSD2 under low Cu(II) availability. (**D**) Same as in (C), but under high Cu(II) availability. The miR398 and U6 signals shown in (C) and (D) are from the same exposure of the same membrane containing both low- and high-Cu(II) samples. (**E**) CIP4 protein and mRNA accumulation, as in (A).

Widespread translational repression by plant miRNAs. Many plant miRNAs, including miR171, target mRNAs within coding sequences, whereas most animal miRNA sites are located in 3′ untranslated regions (3′UTRs). Moreover, SPL3—one of only two examples of plant mRNAs translationally repressed by miRNAs—is targeted in the 3′UTR (*11*–*13*). Consequently, a concern was that the strong effects on protein levels might have been a result of the artificial miR171 target site position in the 3′UTR of GFP171.1, which, moreover, is a constitutively expressed transgene. Therefore, we compared mRNA and protein accumulation of several endogenous miRNA targets, representing all possible target site locations within mRNAs [5′UTR, coding sequence (CDS), and 3′UTR]: two transcription factors targeted by evolutionarily conserved miRNAs (SCL6-IV/miR171/CDS and SPL3/miR156/3′UTR), three stress-related genes also targeted by conserved miRNAs (CSD1/miR398/5′UTR, CSD2/miR398/CDS, and APS1/miR395/CDS), and one target of a nonconserved miRNA known only in *Arabidopsis* (CIP4/miR834/CDS).

mad5 and *mad6* mutants displayed increased protein levels from all these target transcripts. By contrast, both mutants accumulated WT mRNA levels of SCL6-IV, SPL3, CIP4, CSD1, and CSD2 (Fig. 3, A to C and E), although elevated CSD2 mRNA levels were detected in one of three experiments (fig. S2). *mad6*, but not *mad5*, also consistently showed about fourfold higher APS1 mRNA levels (fig. S2). Accumulation of miR171, miR156, and miR398 was unchanged or slightly increased in class III mutants as compared with WT plants (Figs. 2A and 3C), whereas miR395 and miR834 were below the detection limit of Northern analyses (*14*, *15*). Overaccumulation of CSD1 and CSD2, as compared with that in WT plants, was observed in mutant seedlings grown under low Cu(II) availability, allowing miR398 accumulation but not in the presence of high Cu(II) levels, which prevents miR398 expression [Fig. 3, C and D (*16*)]. The correlation between presence of miR398 and deregulation of its targets indicates that class III mutants are specifically affected in miRNA-guided regulation. We note that *dcl1-12* did not exhibit much stronger overaccumulation of CSD1 and SPL3 protein as compared with that observed in *mad5* and *mad6*, despite clear reduction of the corresponding miR398 and miR156 levels. We conclude that (i) translational repression is a widespread mode of plant miRNA action, irrespective of the degree of complementarity or location of target sites within mRNAs; (ii) this process can be genetically uncoupled from miRNA-directed slicing, as in *mad5* and *mad6*; and (iii) certain plant miRNAs exhibiting perfect or near-perfect complementarity to a single target site can repress mRNA expression predominantly at the translation level.

***MAD5* encodes the microtubule-severing enzyme KATANIN.** Positional cloning showed that *mad5* carries a G-to-A transition in the start codon of *KTN1* (Arabidopsis Genome Initiative number:

AT1G80350), causing strongly reduced KTN1 protein levels (Fig. 4A). *KTN1* encodes the P60 subunit of the microtubule-severing enzyme KATANIN. Transformation of *mad5* with a genomic *KTN1* fragment (*17*) restored GFP171.1 silencing (Fig. 4, A and B). Molecular analyses of three previously characterized *ktn1* mutant alleles—*fra2*, *lue1*, and *erh3-3*—showed that each overaccumulates CSD2 and SPL3 proteins without corresponding increases in mRNA levels (Fig. 4C). These results demonstrate that *MAD5* is allelic to *KTN1*. Adenosine Triphosphate (ATP)–dependent microtubule severing is the only known function of KTN1, and because the mutant ktn1 protein produced in *erh3-3* (Fig. 4C) carries a missense mutation in the ATP binding site (*18*, *19*), our data suggest that microtubule dynamics play a role in miRNA-guided translational inhibition but not in miRNA-guided cleavage.

Requirement of the mRNA decapping factor VCS. Components of the decapping complex—DCP1, DCP2, and Ge-1—are required for miRNA-guided translational repression in animals (*20*). Mutations in *Arabidopsis DCP1*, *DCP2*, and the Ge-1 homolog *VCS* are lethal in ecotype Col-0, but as-yet-unidentified modifier loci in ecotype Ler suppress seedling lethality of decapping-deficient *vcs* alleles (*21*, *22*). To test whether plant miRNA–guided translational repression involves components similar to those required in animals, we examined these mutant alleles for miRNA target accumulation. Our analysis included both the homozygous, viable *vcs-1* in Ler, and heterozygous individuals of the seedling-lethal *vcs-7* mutant in Col-0.

vcs-1 mutants exhibited elevated levels of SPL3, SCL6-IV, and CIP4 protein with little or no increase in corresponding mRNA levels (Fig. 5A). No effect was observed on CSD1 and CSD2 protein levels (fig. S3). The *vcs-7* mutation was dominant at the molecular level, despite the recessive seedling lethality phenotype. Thus, *vcs-7* heterozygotes showed overaccumulation of SPL3 and SCL6-IV proteins (fig. S3). In addition, as compared with WT plants, *vcs-7* heterozygotes showed CSD2 protein overaccumulation under low Cu(II) availability, without increases in CSD2 mRNA levels (Fig. 5B). The increased protein levels of miRNA targets in *vcs* mutants were the result of defective miRNA action, because (i) non-miRNA targets (Hsc70, CDC2A) accumulated normally in *vcs* mutants (fig. S3); (ii) CSD2 overaccumulation in *vcs-7* correlated with the presence of miR398 (Fig. 5B); and (iii) upon introgression into the GFP171.1 line, but not into the $GFP_{no\ miR}$ line (both in accession C24), *vcs-7* led to increased GFP protein accumulation in seedlings (Fig. 5, C and D). We conclude that, as in animals, the decapping component VCS is required for miRNA-guided translational repression in plants.

Involvement of AGO1 and AGO10. Next, we asked what AGO protein(s) might be responsible for miRNA-guided translational repression in plants. Four of 10 *Arabidopsis* AGO proteins play established roles in small RNA–directed functions: AGO4 and AGO6 mediate DNA methylation, and AGO7 is involved in biosynthesis of some trans-acting siRNAs, whereas AGO1 can function as a miRNA-guided slicer [reviewed in (*9*)]. AGO2, AGO5, and AGO7 do not interact with most miRNAs (*23*, *24*). Mutations in *AGO10/PNH/ZLL*—the closest paralog of *AGO1*—have been isolated based on their defective shoot apical meristem phenotype (*25*). *ago1* and *ago10* mutants show overlapping developmental defects, and strong alleles are synthetically lethal, suggesting their involvement in similar pathways (*26*). To test the possible role of AGO10 in translational repression, we used the frameshift *ago10* mutant allele, *zll-15* (ecotype Ler). CSD2 mRNA levels were slightly higher in *zll-15* than in WT plants, but CSD2 protein levels were disproportionately higher under low Cu(II) availability (Fig. 6A). CSD2 overaccumulation correlated with the presence of miR398 [as conditioned by Cu(II) availability], and the non-miRNA targets Hsc70 and CDC2A were unaffected, which suggests that this effect is miRNA-dependent (fig. S3). SCL6-IV also showed elevated protein levels in *zll-15*, with SCL6-IV mRNA and miR171 accumulation remaining unchanged (Fig. 6A). The levels of SPL3 were unaffected in *zll-15* (fig. S3), and we did not detect CIP4 in either Ler or *zll-15*. These results suggest that AGO10 is involved in translational repression of only some miRNA targets and that one or several additional AGO protein(s) might contribute to this process.

Hypomorphic *ago1-27* mutants (ecotype Col-0) exhibit near WT accumulation of many miRNA target transcripts, yet display morphological defects similar to *dcl1* mutants (*7*, *27*), suggesting that AGO1 could be involved in translational repression. CSD2 accumulation was increased in *ago1-27*, but this correlated with higher CSD2 mRNA and distinctly lower miR398 levels (fig. S3). By contrast, miR156 and miR171 levels were only moderately reduced in *ago1-27*, whereas the SPL3 and SCL6-IV mRNA levels showed corresponding moderate increases, as compared with those in WT plants (Fig. 6B). Nonetheless, *ago1-27* exhibited disproportionately higher SPL3 and SCL6-IV protein levels. *ago1-27* mutants also displayed elevated CIP4 protein levels with no appreciable difference in mRNA accumulation, but we could not verify any possible effect on miR834 accumulation due to its low abundance. Protein levels of the non-miRNA targets Hsc70 and CDC2A remained unaltered (fig. S3). These results suggest that AGO1 may indeed contribute to miRNA-directed translational repression of SPL3, SCL6-IV, and CIP4 [see also supporting online material (SOM) text].

RNA interference (RNAi) has a translational component in plants. Having established that perfect or near-perfect complementarity is generally compatible with single miRNA species guiding translational repression in plants, we asked whether silencing by populations of siRNAs could also involve translational repression in addition to slicing. To this end, *mad6* and *ago1-27* were introduced into the SUC-SUL (SS) silencing system. In this system, phloem-specific expression of an inverted-repeat (IR) construct triggers non–cell autonomous RNAi of the endogenous mRNA SULFUR (SUL), resulting in a vein-centered chlorotic phenotype. SUL silencing is strictly contingent upon loading of DCL4-dependent 21-nt siRNAs into AGO1

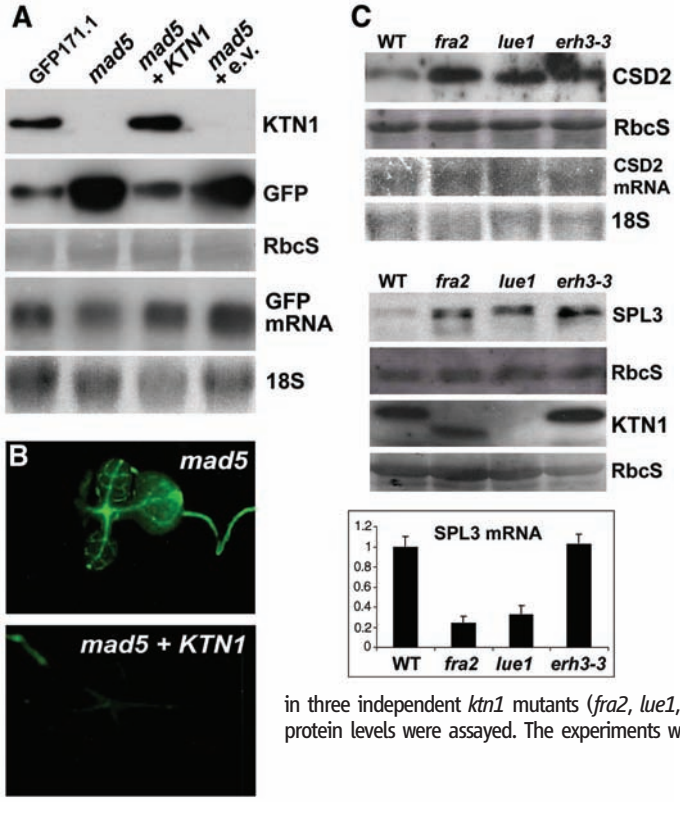

Fig. 4. *MAD5* is allelic to *KTN1*. (**A**) Absence of KTN1 accumulation in *mad5* confirmed by Western analysis. GFP immunoblots showing restoration of miR171-dependent GFP silencing in *mad5* upon transformation with a *KTN1* genomic fragment, but not with empty vector (e.v.). Northern analysis of GFP mRNA levels is shown; 18S rRNA staining provides a loading control. (**B**) GFP fluorescence images of complementation of miR171-dependent GFP silencing upon *KTN1* transformation of *mad5*. (**C**) Accumulation of CSD2 and SPL3 proteins and mRNAs (CSD2: Northern blot; SPL3: quantitative RT-PCR, average ratios ± SD, $n = 3$ PCR replicates) in three independent *ktn1* mutants (*fra2*, *lue1*, and *erh3-3*) in which KTN1 protein levels were assayed. The experiments were performed as in Fig. 3.

(*28*). Therefore, the strong *dcl4-6* mutant was used as a control in those experiments.

The *mad6* and *ago1-27* mutations suppressed SUL silencing (Fig. 6C and fig. S4). Molecular analyses of *mad6* showed a strong decrease in SUL siRNA accumulation, accompanied by a mild increase in SUL mRNA. Nonetheless, SUL protein levels were appreciably higher than those in the SS reference line (fig. S4), which suggests that SUL silencing does not rely exclusively on mRNA degradation. In *ago1-27*, the SUL siRNA levels were unchanged as compared with those in the parental SS line (Fig. 6D), and SUL mRNA levels were nearly as low in *ago1-27* as they were in the parental SS line. SUL protein levels, however, were clearly higher in *ago1-27* mutants (Fig. 6D). This represented suppression of SUL silencing because, without the SS transgene, SUL protein levels were unchanged in *ago1-27* plants as compared with WT plants (fig. S4). We conclude that the hairpin-derived SUL siRNA population mediates translational repression in addition to mRNA degradation.

Discussion. Imperfect pairing with central mismatches in small RNA–target hybrids promotes translational repression because it excludes slicing. It is a common inference that, conversely, near-perfect complementarity excludes translational repression because it enables slicing. This has contributed to the notion that plant and animal miRNAs act in fundamentally different ways. Our finding of a general translational component in plant miRNA and siRNA action demonstrates this inference to be erroneous and provides a genetic foundation to several key observations. First, translational repression by near-perfectly matched miRNAs has been reported twice in *Arabidopsis* (*11*–*13*). Although regarded as exceptions, those examples may well define a stereotype of plant small RNA action. Second, artificial miRNAs can produce phenotypes indistinguishable from genetic knockouts of their targets, despite incomplete target mRNA reduction (*29*). Third, experiments with an inducible RNAi construct identified an extended time window during which target mRNA had returned to its original levels, while protein activity remained suppressed (*30*).

We propose that translational repression is the default mechanism by which small RNAs silence messages, both in plants and animals. Near-perfectly matched small RNAs may in addition engage in slicing such that their regulatory output results from a combination of both mechanisms. The CIP4-miR834 interaction demonstrates that, while necessary, near-complete pairing is not sufficient for slicing to contribute substantially to silencing in plants. miR834 is part of a large group of recently identified nonconserved ("young") miRNAs, many of which are presumed to be nonfunctional because their putative target mRNA levels are unchanged in *dcl1* and *hen1* mutants (*31*). Rather, inspection of the CIP4 protein levels suggests that such young miRNAs might be primarily channeled to translational inhibitory pathways. Nonetheless, these examples do not undermine the importance of slicing in plant biology: The pronounced morphological defects of slicer-deficient *ago1* mutants (SOM text) and *mad1→mad4* mutants, as compared with the mild developmental phenotype of *mad5* and *mad6*, suggest that miRNA-guided slicing, not translational inhibition, is indispensable for plant development (fig. S5).

Differences in position, number, and pairing degree of miRNA target sites have been used to substantiate contrasted views of plant and animal miRNA action. However, the unbiased genetic analysis conducted here shows that these features have little or no influence on either the mode or efficiency of miRNA-directed repression. The premise that miRNAs in plants act mostly via slicing has prompted the use of near-perfect complementarity as the exclusive criterion for identification of plant miRNA targets (*14*, *31*, *32*). Our results suggest that the existence of extensively mismatched miRNA targets regulated mostly at the protein level now warrants serious consideration (*33*). Studies of many rice "orphan" miRNAs with no obvious complementary target transcripts could provide a means to investigate this important issue (*34*). Finally, because hairpin-derived siRNA populations in plants act partially via translational inhibition, it is conceivable that the same is true of plant viral siRNAs, which are thought to confer immunity mainly via slicing. The possibility also emerges that RNAi in animals might generally involve translational repression: In one example of RNAi in Sertoli cells, the siRNA target was indeed repressed exclusively at the protein level (*35*).

The finding that AGO1 may concurrently slice and translationally inhibit a given mRNA pool raises the question of how slicing is avoided during translational inhibition. It also remains unclear whether the two mechanisms coexist within the same cells, or whether they can be spatially and/or temporally separated. Tissue specificity of plant miRNA and target expression could also influence the prevalence of one process over the other. The identification of *MAD5* as *KTN1* suggests that dynamic reorganization of the microtubule network is important for miRNA-directed translational re-

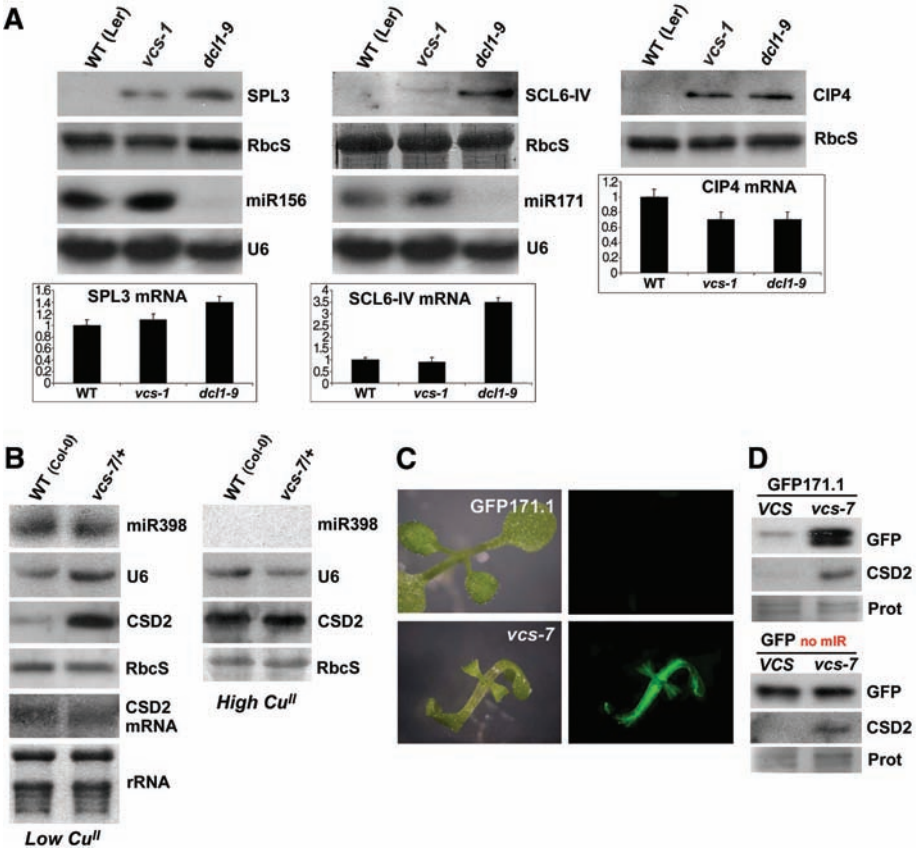

Fig. 5. miRNA target protein and mRNA accumulation in *vcs* mutants. (**A**) Accumulation of target proteins and mRNAs (SPL3, SCL6-IV, and CIP4) corresponding to miR156, miR171, and miR834 in *vcs-1* homozygotes as compared with WT and *dcl1-9* plants. Coomassie-stained RbcS provides a loading control. For real-time RT-PCR analysis of SPL3, SCL6-IV, and CIP4 mRNAs, cDNA inputs were normalized to 18S rRNA. Gene expression ratios are relative to the WT levels (Ler) and shown as averages ± SD (n = 3 PCR replicates). (**B**) Accumulation of miR398, as well as mRNA and protein of its target CSD2, as in Fig. 3, C and D. (**C**) Phenotypes (left images) and GFP fluorescence (right images) of VCS and *vcs-7* homozygotes introgressed into the GFP171.1 background at 14 days of growth. (**D**) (Top panel) GFP accumulation in seedlings depicted in (C). (Bottom panel) Same as in Fig. 2C upon introgression of $GFP_{no\ miR}$. Differential accumulation of CSD2 (miR398 target) confirms the presence of the *vcs-7* mutation [low Cu(II)]. Prot, Coomassie-stained bands that serve as a loading control.

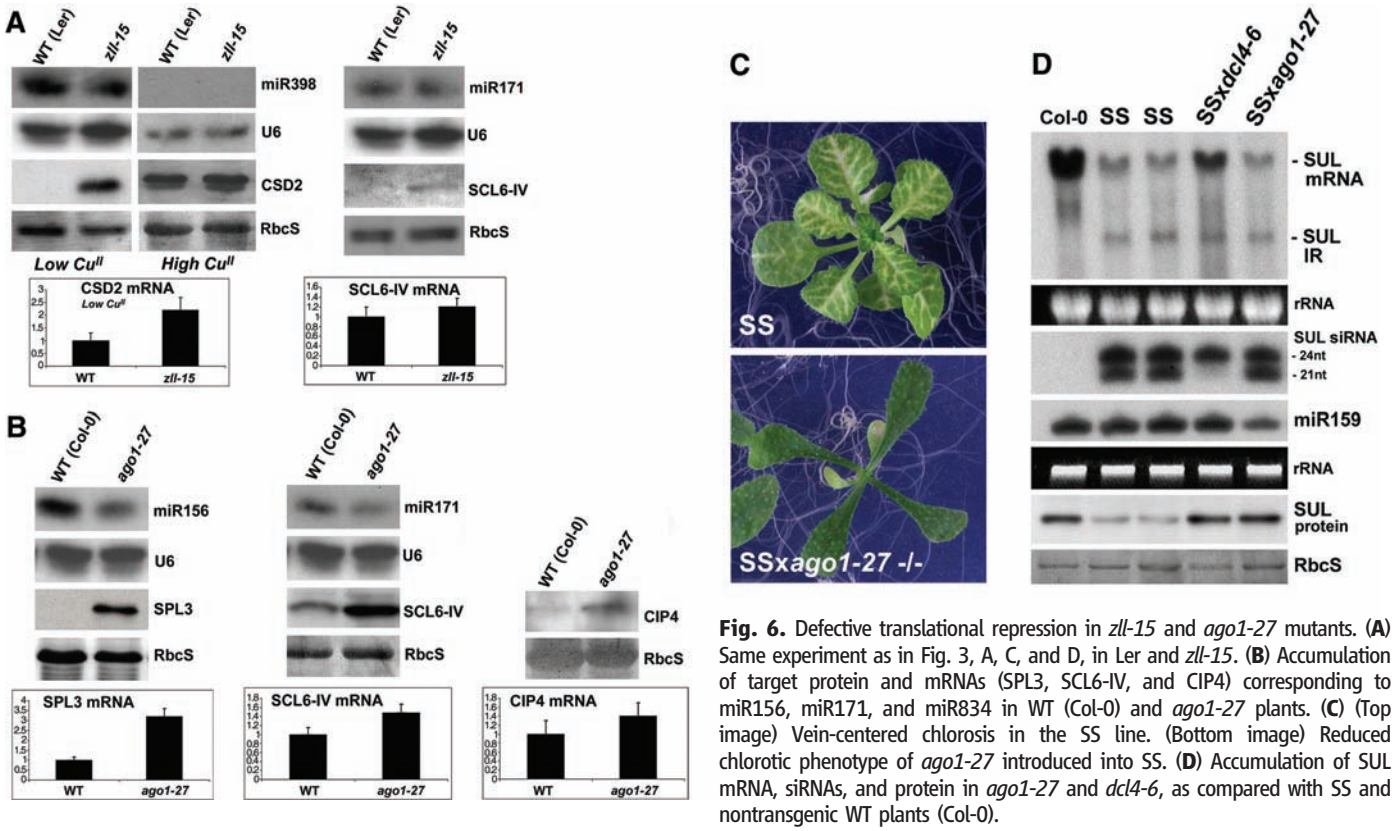

Fig. 6. Defective translational repression in *zll-15* and *ago1-27* mutants. (**A**) Same experiment as in Fig. 3, A, C, and D, in Ler and *zll-15*. (**B**) Accumulation of target protein and mRNAs (SPL3, SCL6-IV, and CIP4) corresponding to miR156, miR171, and miR834 in WT (Col-0) and *ago1-27* plants. (**C**) (Top image) Vein-centered chlorosis in the SS line. (Bottom image) Reduced chlorotic phenotype of *ago1-27* introduced into SS. (**D**) Accumulation of SUL mRNA, siRNAs, and protein in *ago1-27* and *dcl4-6*, as compared with SS and nontransgenic WT plants (Col-0).

pression and is supported by several lines of evidence: RNAi of tubulins in *Caenorhabditis elegans* compromises target regulation by distinct miRNAs (*36*), whereas *Drosophila* Armitage, which is required for RISC assembly, is a microtubule-associated protein (*37*), as are FMR (necessary for miRNA-directed translational activation) and the ribosome-interacting AGO-like protein Seawi (*38*–*40*). Finally, many mRNA decay factors that colocalize with the decapping complex in cytoplasmic processing (P) bodies interact with tubulin or with microtubule polymers in yeast (*41*, *42*). Identifying the P-body component VCS as integral to nondegradative translational repression in plants is important in two respects. First, it reveals some level of mechanistic similarity between plant and animal miRNA-mediated repression. Second, it suggests that RNA decay could be coupled to the action of at least some plant miRNAs, as established in animal cells (*20*, *43*). An outstanding question pertains to the biological importance of translational inhibition in plants. Studies on human cells suggest that one key aspect lies in the reversible nature of this type of regulation (*44*). This may be particularly adapted to coordination and resetting of stress-responsive gene expression, an emerging function of many plant miRNAs (*45*).

References and Notes

1. D. P. Bartel, *Cell* **116**, 281 (2004).
2. G. Hutvagner, P. D. Zamore, *Science* **297**, 2056 (2002).
3. J. J. Song, S. K. Smith, G. J. Hannon, L. Joshua-Tor, *Science* **305**, 1434 (2004).
4. M. W. Jones-Rhoades, D. P. Bartel, B. Bartel, *Annu. Rev. Plant Biol.* **57**, 19 (2006).
5. Y. Qi, A. M. Denli, G. J. Hannon, *Mol. Cell* **19**, 421 (2005).
6. N. Baumberger, D. C. Baulcombe, *Proc. Natl. Acad. Sci. U.S.A.* **102**, 11928 (2005).
7. H. Vaucheret, F. Vazquez, P. Crete, D. P. Bartel, *Genes Dev.* **18**, 1187 (2004).
8. E. A. Parizotto, P. Dunoyer, N. Rahm, C. Himber, O. Voinnet, *Genes Dev.* **18**, 2237 (2004).
9. E. J. Chapman, J. C. Carrington, *Nat. Rev. Genet.* **8**, 884 (2007).
10. C. Llave, Z. Xie, K. D. Kasschau, J. C. Carrington, *Science* **297**, 2053 (2002).
11. X. Chen, *Science* **303**, 2022 (2004).
12. M. J. Aukerman, H. Sakai, *Plant Cell* **15**, 2730 (2003).
13. M. Gandikota *et al.*, *Plant J.* **49**, 683 (2007).
14. M. W. Jones-Rhoades, D. P. Bartel, *Mol. Cell* **14**, 787 (2004).
15. R. Rajagopalan, H. Vaucheret, J. Trejo, D. P. Bartel, *Genes Dev.* **20**, 3407 (2006).
16. H. Yamasaki *et al.*, *J. Biol. Chem.* **282**, 16369 (2007).
17. T. Bouquin, O. Mattsson, H. Naested, R. Foster, J. Mundy, *J. Cell Sci.* **116**, 791 (2003).
18. V. Stoppin-Mellet, J. Gaillard, M. Vantard, *Plant J.* **46**, 1009 (2006).
19. M. Webb, S. Jouannic, J. Foreman, P. Linstead, L. Donan, *Development* **129**, 123 (2002).
20. A. Eulalio *et al.*, *Genes Dev.* **21**, 2558 (2007).
21. J. Xu, J. Y. Yang, Q. W. Niu, N. H. Chua, *Plant Cell* **18**, 3386 (2006).
22. D. C. Goeres *et al.*, *Plant Cell* **19**, 1549 (2007).
23. S. Mi *et al.*, *Cell* **133**, 116 (2008).
24. T. A. Montgomery *et al.*, *Cell* **133**, 128 (2008).
25. B. Moussian, H. Schoof, A. Haecker, G. Jurgens, T. Laux, *EMBO J.* **17**, 1799 (1998).
26. K. Lynn *et al.*, *Development* **126**, 469 (1999).
27. J.-B. Morel *et al.*, *Plant Cell* **14**, 629 (2002).
28. P. Dunoyer, C. Himber, V. Ruiz-Ferrer, A. Alioua, O. Voinnet, *Nat. Genet.* **39**, 848 (2007).
29. R. Schwab, S. Ossowski, M. Riester, N. Warthmann, D. Weigel, *Plant Cell* **18**, 1121 (2006).
30. C. Lo, N. Wang, E. Lam, *FEBS Lett.* **579**, 1498 (2005).
31. N. Fahlgren *et al.*, *PLoS One* **2**, e219 (2007).
32. Y. Zhang, *Nucleic Acids Res.* **33**, W701 (2005).
33. D. V. Dugas, B. Bartel, *Plant Mol. Biol.* published online 8 April 2008; 10.1007/s11103-008-9329-1.
34. J. F. Wang, H. Zhou, Y. Q. Chen, Q. J. Luo, L. H. Qu, *Nucleic Acids Res.* **32**, 1688 (2004).
35. M. K. Rao *et al.*, *Genes Dev.* **20**, 147 (2006).
36. D. H. Parry, J. Xu, G. Ruvkun, *Curr. Biol.* **17**, 2013 (2007).
37. H. A. Cook, B. S. Koppetsch, J. Wu, W. E. Theurkauf, *Cell* **116**, 817 (2004).
38. S. Vasudevan, Y. Tong, J. A. Steitz, *Science* **318**, 1931 (2007).
39. A. J. Rodriguez *et al.*, *RNA* **11**, 646 (2005).
40. H. Wang *et al.*, *Mol. Biol. Cell* **19**, 105 (2007).
41. J. Liu *et al.*, *Nat. Cell Biol.* **7**, 1261 (2005).
42. A. C. Gavin *et al.*, *Nature* **440**, 631 (2006).
43. A. J. Giraldez *et al.*, *Science* **312**, 75 (2006).
44. S. N. Bhattacharyya, R. Habermacher, U. Martine, E. I. Closs, W. Filipowicz, *Cell* **125**, 1111 (2006).
45. R. Sunkar, V. Chinnusamy, J. Zhu, J. K. Zhu, *Trends Plant Sci.* **12**, 301 (2007).

46. This work was supported by grants from the European Molecular Biology Organization (ALTF-251 2004) and the European Union (EIF 25064 2005) to P.B., as well as by grants "MicroTRAC" from l'Agence Nationale de la Recherche/Genoplante, "SIROCCO" LSHG-CT-2006-037900 from the European Union, and an Action Thématique Incitative sur Programme Plus from CNRS to O.V. We thank D. Kliebenstein (CSD1, CSD2), P. Huijser (SPL3), T. Leustek (APS), P. E. Jensen (ChlI/SUL), and M. Vantard (KTN1) for antibodies; Z. Ye (*fra2*), J. Mundy (*lue1*), L. Dolan (*erh3-3*), and T. Laux (*zll-15, ago1-27*) for seeds; C. Himber for help with *ago1-27* × SS experiments and plant pictures; and R. Wagner's team for plant care.

Supporting Online Material

www.sciencemag.org/cgi/content/full/1159151/DC1
Materials and Methods
SOM Text
Figs. S1 to S6
Table S1
References

15 April 2008; accepted 1 May 2008
Published online 15 May 2008;
10.1126/science.1159151
Include this information when citing this paper.